



The Society shall not be responsible for statements or opinions advanced in papers or in discussion at meetings of the Society or of its Divisions or Sections, or printed in its publications. Discussion is printed only if the paper is published in an ASME Journal. Released for general publication upon presentation. Full credit should be given to ASME, the Technical Division, and the author(s). Papers are available from ASME for nine months after the meeting.
Printed in USA

Copyright © 1982 by ASME

Jet-Wake Analysis for Centrifugal Compressor Static Pressure Rise and Deviation Angle

R. C. Pamphreen

Manager,
Advanced Aero Systems,
Williams International,
Walled Lake, MI
Mem. ASME

This paper discusses the static pressure recovery characteristics of four different centrifugal compressor impellers. Comparison is made to effectiveness values obtained with rectangular and conical diffuser data. Effectiveness levels comparable to the diffuser data occur up to the point of maximum flowpath curvature. In the radial portion of the impellers, rotation affects static pressure recovery. Also presented are values of rotor exit deviation angle deduced from the jet-wake analysis of these four impellers. It was found that deviation angle is only a function of blade exit angle. The sensitivity of the value of calculated deviation angle to the magnitude of assumed aerodynamic blockage is discussed. For the jet-wake model, the deviation angle is zero for blade exit angles of thirty degrees.

NOMENCLATURE

DR diffusion ratio
g gravitational acceleration, m/s/s
H total enthalpy, cal/kg
h static enthalpy, cal/kg
J work equivalent of heat, kg-m/cal
 P_1 static pressure at throat center on 50% massflow streamsheet, kPa
 P_2 static pressure at rotor exit, kPa
 R_2 rotor exit radius, m
 V_θ absolute tangential velocity, m/sec
W relative velocity, m/sec
 ϵ_1 Eq. 5 with W_2 = suction surface minimum velocity
 ϵ_2 Eq. 5 with W_2 = rotor exit velocity
 ω rotational speed, rads/sec

From Ref. 1

R_i Richardson No., dimensionless, $= \omega B / W_{\min}$
B blockage at point of actual minimum velocity, m
 W_{\min} suction surface actual minimum velocity, m/s
 W_{\max} suction surface actual maximum velocity, m/s
 P_B $M^2 \left[(a/R_a) + (2\omega a/W) \sin \delta \right]$ = blade acceleration parameter

P_F $M^2 \left[(b/R_b) \cos^2 \beta + (2\omega b/W) \sin \beta \cos \delta \right]$ = flowpath acceleration parameter
 P_D $M^2 (W_{\max} - W_{\min}) / W_{\max}$ = diffusion parameter
a blade spacing at maximum curvature, m
b flowpath width at maximum curvature, m
 R_a blade radius of curvature, m
 R_b meridional radius of curvature, m
 β relative flow direction, degrees
 δ meridional streamline direction, degrees

From Ref. 7

δ deviation angle, degrees $= \frac{m}{\sqrt{\sigma}} (\beta_{B_1} - \beta_{B_{2EQ}})$
m deviation angle coefficient
 σ solidity $= LN_B / \pi (R_{m_1} + R_T)$
(nomenclature section of Ref. 7 incorrectly shows π multiplied by 2.)
L length of flowpath meanline, m
 N_B number of blades
 R_{m_1} inlet arithmetic mean radius, m
 R_T outlet radius, m
 β_{B_1} blade angle at R_{m_1} , degrees
 $\beta_{B_{2EQ}}$ equivalent exit blade angle of a two-dimensional blade having same circulation as centrifugal compressor blade

SUBSCRIPTS

| | | | |
|-----|-------------|-----|---------|
| 1 | rotor inlet | id | ideal |
| 2 | rotor exit | max | maximum |
| act | actual | min | minimum |

¹Work was performed during previous employment at Chrysler Corporation. Contributed by the Gas Turbine Division of the ASME.

INTRODUCTION

The jet-wake flow model of centrifugal compressor impellers is analogous to the flow in stationary diffusers in the sense that there is a potential core surrounded by a developing and possibly separated boundary layer. Centrifugal compressor impellers, however, have flowpath meridional and blade curvatures and Coriolis acceleration influencing static pressure recovery as well as flow area increase. An assessment is made in (1) of the impact of these influences on the development of blockage through four experimental impellers. Evaluation of the importance of the constituent influences showed that blockage in the axial-radial bend of the rotor is about equally determined by diffusion, flowpath curvature, and the combined effect of blade curvature and Coriolis acceleration. Thus, diffusion and flowpath curvature are twice as influential as blade curvature and Coriolis acceleration on blockage growth.

As an extension of the work reported in (1) and to appreciate the influence of impeller geometry on static pressure recovery, this paper presents a review of the effectiveness values achieved by the impellers analyzed in (1). The values of static pressure and kinetic energy used to compute effectiveness values in this paper were taken from the jet-wake analysis reported in (1). Comparison is made to effectiveness levels achieved in stationary diffusers and to the influence of blade incidence angle, which is not a factor in stationary diffuser recovery, but is a natural influence on impeller performance.

This paper also presents values of rotor exit deviation angle deduced from the jet-wake analysis of the four impellers reported in (1). This information is presented to show the values of deviation angle to expect with the jet-wake theory as a result of the analysis carried out in (1).

BACKGROUND

Data for this study came from two radial-bladed and two backswept impellers. Table 1 shows a summary of design information. Instrumentation and data uncertainties are discussed in detail in (1).

Static pressure recovery is based on the throat center static pressure of the 50% massflow streamsheet. Local static pressure and velocity were determined from streamline curvature, radial equilibrium calculations in which the shroud static pressure was made equal to experimental data by specifying sufficient local blockage. Ideal values were computed for potential flow conditions with zero blockage. Deviation angle at the rotor exit was determined by iteratively adjusting blockage and deviation angle values until the mass-averaged temperature matched measured data within $\pm 0.5^\circ\text{C}$ and the tip-static/inlet-total pressure ratio matched the data within 0.003. Blade surface velocities were computed from the assumption of zero absolute rotational motion and a linear distribution of velocity between pressure and suction surfaces.

IMPELLER DIFFUSION PERFORMANCE

Calculations were performed to compare the actual to the ideal values of diffusion ratio and to determine the effectiveness values of the impeller static pressure rise. The diffusion ratio, DR, is defined as the amount of velocity decrease as a fraction of maximum velocity. Thus,

$$DR = (W_{\max} - W_{\min})/W_{\max} = 1 - (W_{\min}/W_{\max}) \quad (1)$$

The velocities used are the suction surface velocities on the 50% massflow streamsheet. The effectiveness is defined as the ratio of the actual to the ideal static pressure rise in the impeller. Thus,

$$\epsilon = (P_2 - P_1)_{\text{act}} / (P_2 - P_1)_{\text{id}} \quad (2)$$

where the numerator is the actual rise, and the denominator is the ideal rise. The pressures used are the throat-center pressure for P_1 and the rotor exit pressure for P_2 . Note that the effectiveness is for the overall static pressure rise of the rotor, but the diffusion ratio is referenced to the minimum suction surface velocity, which generally was not at the rotor exit for these impellers.

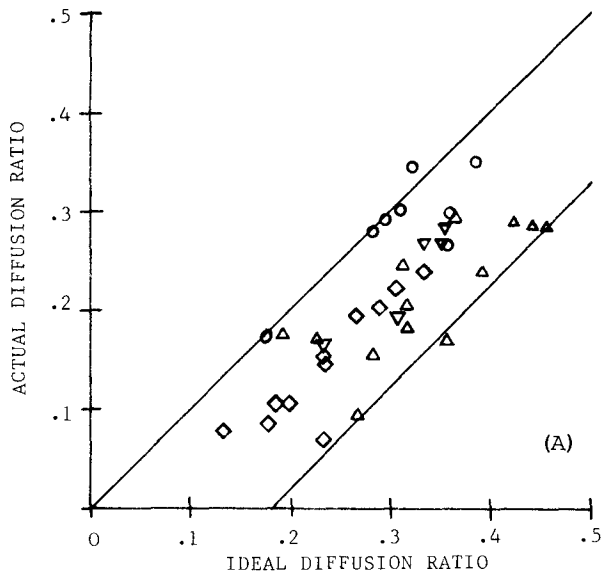
Fig. 1A shows the comparison of actual to ideal diffusion ratios. The spread of the group of points, as defined by the straight lines, is 0.16 in units of actual diffusion ratio at any given value of ideal diffusion ratio. Except for Impeller A, the trend of the group of points is for actual diffusion ratio to be less than the ideal value.

Fig. 1B isolates the range of points for the two backswept impellers. Within this range the actual diffusion ratio only varies 0.04 or just one-fourth the spread shown by the radial impellers. The high values of actual diffusion ratio for Impeller A are attributed to a sharp reduction in blockage at the splitter leading edge, as shown in Fig. 4 of (1). The other splitttered radial impeller and the two backswept impellers had progressive increases in blockage from the rotor leading edge. If we consider Impeller A as an exception, the trend shown in Fig. 1B shows higher values of actual diffusion ratio for the two backswept impellers than for radial Impeller C. This could be a generally accepted result since it is commonly felt that backward curvature provides better control of blade loading than radial blading does.

Fig. 2 shows the values of effectiveness obtained for the four impellers plotted against incidence angle at the 50% massflow streamline. This plot can be compared against the results shown by Kenny in (2). The maximum values are lower than those presented in (2), and the fall off at negative incidence angles depends on the impeller choke characteristic. The throat blockage varied from 2% to 8%, with one value of 16%. In his paper, Kenny presents the effectiveness of the impeller static pressure rise as a function of throat blockage. Contrary to the results presented in (2), the effectiveness could not be simply correlated against throat blockage. This is to be expected since, for the impellers analyzed herein, there are major increases in blockage near the axial-radial bend of the flowpath, which are due to diffusion, curvature and Coriolis effects. Based on the analysis of (1) and on the test results with laser velocimetry and low-speed probing as reviewed in (1), it should be considered doubtful that the static pressure rise through an impeller could be simply related to throat blockage.

It must be noted, however, that the impeller static pressure rise is due not only to the diffusion of the relative velocity but also to the increase of potential energy due to centrifugal force. As Johnston (3) points out, the centrifugal force is a conservative force since it can be written as a gradient of a scalar potential. Hence, it should not have an influence on the stability of the boundary layer.

| | | | | |
|-------------------------------------------|---|---|---|---|
| IMPELLER | A | B | C | D |
| SYMBOL | ○ | ◇ | △ | ▽ |
| DIFFUSION RATIO = $1 - (W_{MIN}/W_{MAX})$ | | | | |



| | | | | |
|-------------------------------------------|---|---|---|---|
| IMPELLER | A | B | C | D |
| SYMBOL | ○ | ◇ | △ | ▽ |
| DIFFUSION RATIO = $1 - (W_{MIN}/W_{MAX})$ | | | | |

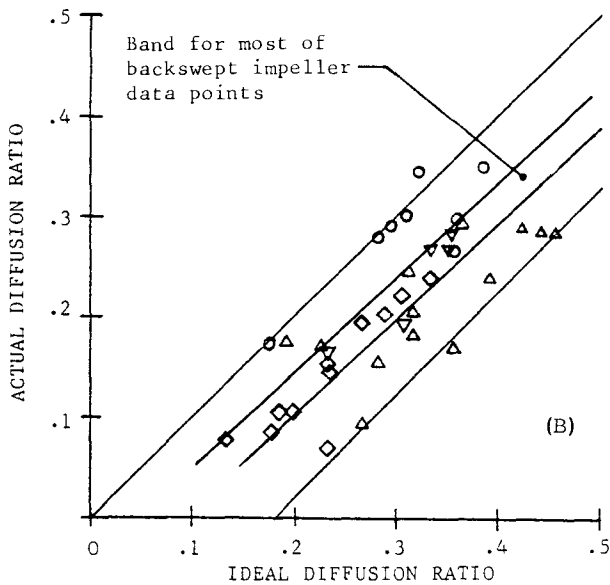


Fig. 1 Variation of actual versus ideal diffusion ratio on blade suction surface of 50% massflow stream-sheet

TABLE 1

| | | | | |
|------------------------------------|-----|-----|-----|-----|
| Impeller | A | B | C | D |
| Design speed, rpm $\times 10^{-3}$ | 50 | 46 | 50 | 50 |
| Design flow, kg/sec. | 1.2 | 0.9 | 1.3 | 1.3 |
| No. of full blades | 15 | 18 | 16 | 24 |
| No. of splitters | 15 | 0 | 16 | 0 |
| Exit blade angle, degrees | 0 | 30 | 0 | 30 |

In (4), for instance, the static pressure recovery is based on the value of pressure obtained by subtracting out the contribution due to centrifugal force.

A slightly different treatment is needed for the compressible flow in an impeller. For zero inlet swirl, the impeller exit stagnation enthalpy is

$$H_2 = H_1 + \omega R_2 V_{\theta 2} / gJ \quad (3)$$

If we substitute $H = h + V^2/2gJ$ and $U = \omega R + W_{\theta}$ into Eq. (3), we get, after algebraic manipulation,

$$2gJ(h_2^* - h_1^*)/W_1^2 = 1 - (W_2/W_1)^2 \quad (4)$$

where

$$h^* = h - \omega^2 R^2 / 2gJ$$

If we now define effectiveness as

$$\epsilon = (h_2^* - h_1^*)_{act} / (h_2^* - h_1^*)_{id}$$

then,

$$\epsilon = [1 - (W_2/W_1)^2]_{act} / [1 - (W_2/W_1)^2]_{id} \quad (5)$$

This definition is a ratio of the actual to the ideal reduction in kinetic energy. In analyzing impeller performance, we can consider effectiveness of suction-surface diffusion from maximum velocity to minimum velocity or from maximum velocity to the impeller exit velocity. Both of these definitions are reviewed here.

| | | | | |
|----------|---|---|---|---|
| IMPELLER | A | B | C | D |
| SYMBOL | ○ | ◇ | △ | ▽ |

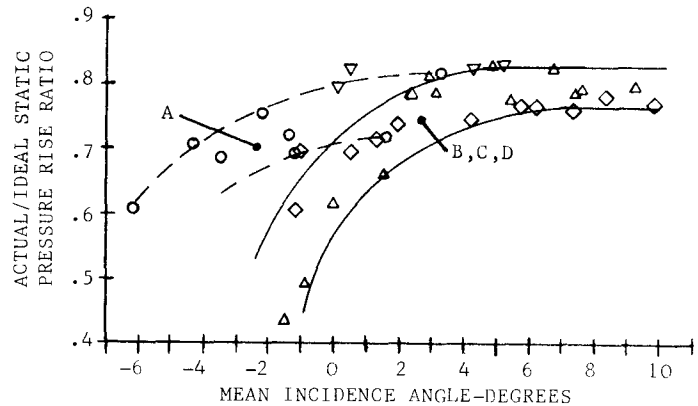


Fig. 2 Variation of actual/ideal static pressure rise ratio as a function of incidence angle, on suction surface of 50% massflow stream-sheet

Fig. 3 shows the variation of actual/ideal relative kinetic energy reduction, ϵ_1 , from maximum to minimum velocity on the suction surface of the 50% massflow stream-sheet as a function of incidence angle. The effectiveness values of Impellers B, C and D fall into one group in which effectiveness varies with incidence angle. The values for Impeller A are much higher and show little variation with incidence angle.

If we again consider the results of Impeller A as an exception, the maximum values of effectiveness shown by the other impellers very between 0.66 and 0.84. This is the range of effectiveness values achieved in conical diffusers (5) for included angles between 2° and 15° and in rectangular diffusers between 2° and 10° with 5% inlet blockage (6) and area ratio less than 2.5:1.

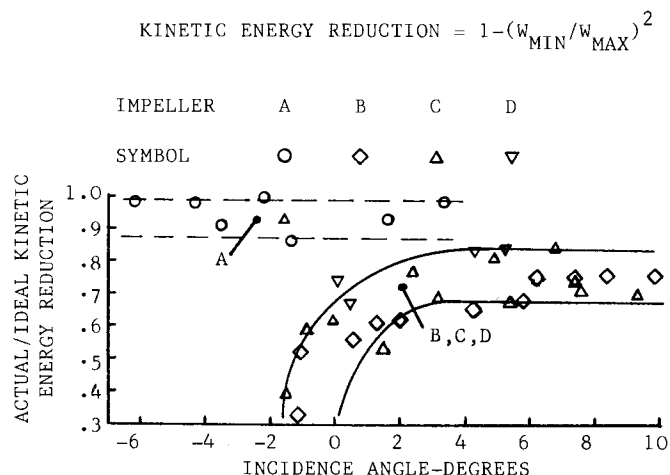


Fig. 3 Variation of actual/ideal relative kinetic energy reduction from maximum to minimum velocity on suction surface of 50% massflow streamsheet as a function of incidence angle.

Fig. 4 shows the variation of actual/ideal relative kinetic energy reduction, ϵ_2 , from maximum to rotor-exit velocity on the suction surface of the 50% massflow streamsheet as a function of incidence angle. The effectiveness values of Impellers C and D are higher than those of Impellers A and B by approximately 0.3 units. The difference in ϵ_2 between Impellers C and D and Impeller B can be attributed to Richardson number differences. Fig. 5 shows a plot of blockage increase in the radial portion of the impeller versus Richardson number. This is the same plot as Fig. 9 in (1). However, the symbols are changed to identify the points for the different impellers. The figure shows that the points for Impeller B are generally at higher values of Richardson number and have generally higher values of blockage increase compared to the points for Impellers C and D. Impeller A is again an anomaly since it has points at low Richardson number but also low values of ϵ_2 .

DEVIATION ANGLE RESULTS

In carrying out the blockage analysis, it was explained in (1) that the experimental values of rotor tip static pressure and the exit temperature were matched by concurrently varying exit blockage and deviation angle until calculation values matched test values. This section presents the resultant values of deviation angle obtained from the data match calculations with the four impellers used in this analysis. No assumption was made for the possible contribution of windage to the rotor temperature rise.

It was shown in (1) that the blockage development

up to the point of minimum velocity depended on the total acceleration parameter, AP. It was therefore considered appropriate to check if deviation angle was influenced by acceleration parameter. The deviation angle values obtained from the four impellers are plotted against acceleration parameter in Fig. 6. The results show that, within data scatter, deviation angle is only a function of blade exit angle and not the acceleration parameter. This suggests that deviation angle obtained for the jet-wake flow model is only determined by blade exit angle and not by aerodynamic conditions upstream of the trailing edge within the blade passage.

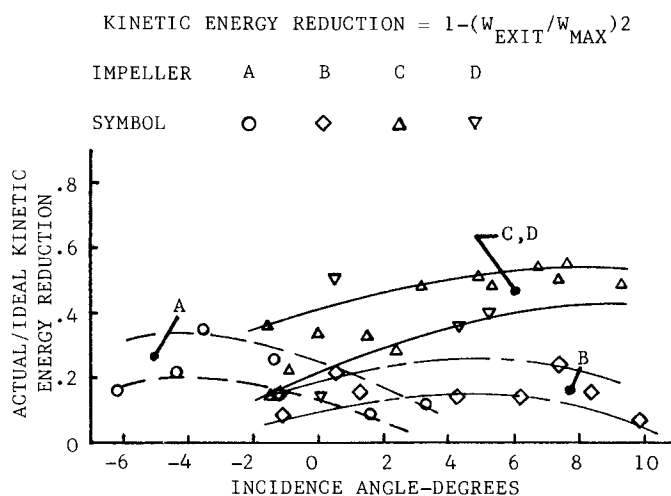


Fig. 4 Variation of actual/ideal relative kinetic energy reduction from maximum to rotor-exit velocity on suction surface of 50% massflow streamsheet as a function of incidence angle.

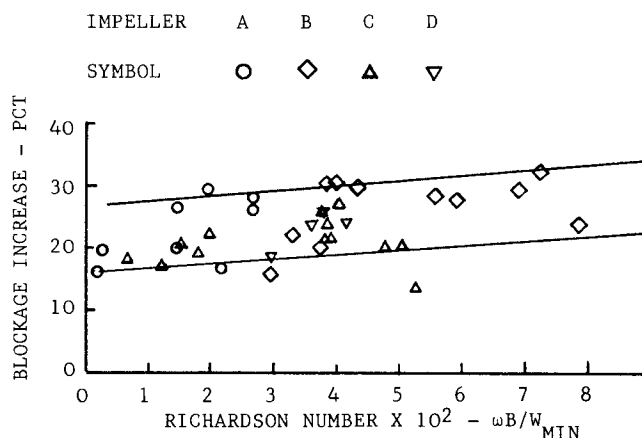


Fig. 5 Variation of blockage increase from point of minimum velocity to the rotor exit as a function of Richardson Number.

This result is in contrast to the analysis presented in (7), which showed that deviation angle coefficient, m , varies with the amount of suction-surface shroudline diffusion (Fig. 12 in (7)). The vector diagrams used for computing deviation angle in (7) were based on the assumption of 10% blockage. The deviation angle coefficient computed with 10% blockage for data points used in the present analysis are computed with those of (7) and shown in Fig. 7. The plot shows separate bands of data for the radial and back-swept impellers. For each impeller type, the deviation angle coefficient is almost independent of diffusion ratio except at very low values.

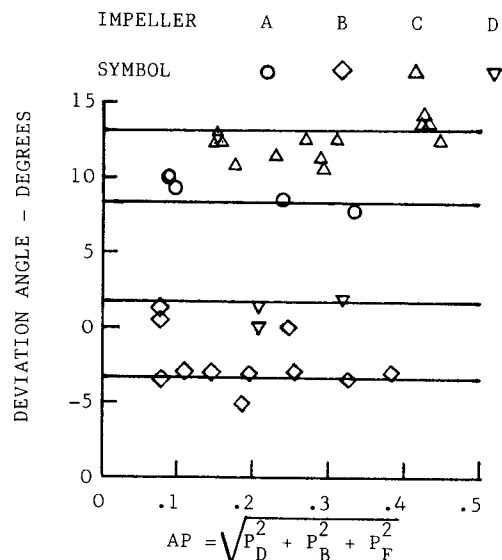


Fig. 6 Variation of deviation angle with acceleration parameter.

However, the values of deviation angle and of deviation angle coefficient depend on the blockage assumption. If deviation angle is computed with jet-wake-model blockage, the deviation angle and the coefficient will be lower. Deviation angle coefficient values obtained from the jet-wake-model are plotted against shroudline diffusion ratio in Fig. 8. The plot shows deviation angle coefficient to be independent of diffusion ratio and to be dependent only on rotor exit blade angle.

It must be concluded, therefore, that the deviation angle is only a function of rotor exit angle, whether 10% blockage is assumed or whether the jet-wake model is used. The amount of deviation angle depends on the blockage model. The backswept rotors used here all had 30 degrees exit angle. Fig 7 suggests that data bands can be created for other values of backsweep if linear interpolation and extrapolation can be assumed. For the jet-wake model, however, zero deviation angle could be assumed for blade exit angles of 30 degrees or larger.

The designer is now faced with two models. If he uses the more familiar approach with 10% blockage, deviation angle can be computed from Fig. 7 and the equations in (7). It should be noted that some designers use only 5% blockage, and some use none at all. If the designer uses the jet-wake model, zero deviation can be used for blade exit angles of 30° or more.

More importantly, however, is the question of the model which more correctly reflects the true fluid mechanic conditions. The list of references cited in

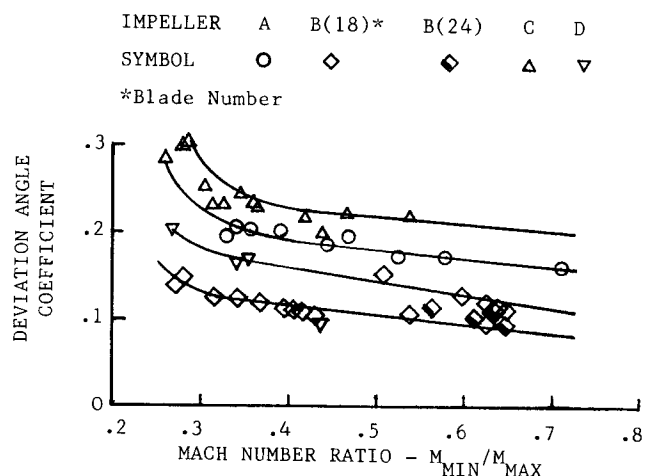


Fig. 7 Variation of deviation angle coefficient with ideal suction-surface tip-streamline Mach Number ratio - 10% blockage assumed at rotor exit.

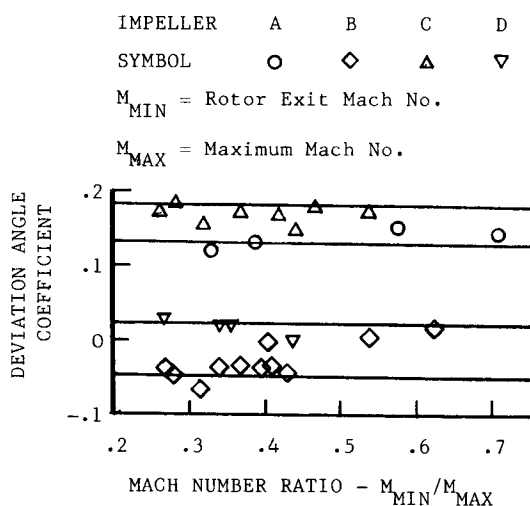


Fig. 8 Variation of deviation angle for jet-wake flow model with ideal suction-surface tip-streamline Mach Number ratio

(1) presents a strong argument in favor of the jet-wake model. Furthermore, the only deviation from ideal flow conditions for backswept impellers with 30° blade angle or larger is the presence of aerodynamic blockage. Otherwise, the core flow has zero loss and follows the blade direction throughout the channel up to and including the trailing edge. Furthermore, development of the model lies in determining the distribution of blockage from hub to shroud. For a model which contains loss as well as blockage, additional work is needed to determine the relative magnitudes of loss and blockage as well as the respective distributions from hub to shroud. However, at present, flow visualization and inter-blade measurements more closely support a model with blockage and a potential core.

CONCLUSION

Values of static pressure effectiveness and deviation angle, computed from the jet-wake model, have been presented for four completely different impeller designs. Except for one impeller, the maximum values of effectiveness were consistent with diffuser data for that portion of the impeller from the inlet to the point of ideal minimum velocity, which occurred at or near the meridional flowpath maximum curvature. Except for the same impeller, overall impeller effectiveness was further influenced by the magnitude of the Richardson number. The one impeller showed anomalies which could not be explained.

From the jet-wake model analysis, it was found that deviation angle is only a function of blade exit angle. Deviation angle for the backswept impellers was, within data scatter, virtually zero. The deviation for the two radial impellers was about 10° . This result differs from the results presented in (7), which were based on 10% blockage. With additional data supplied from the data used herein, separate bands of data can be identified for the deviation angle coefficient for the radial impellers and for the backswept impellers. Furthermore, this coefficient is virtually independent of shroudline diffusion ratio, which differs from the results shown in (7).

REFERENCES

- 1 Pampreen, Ronald C., "A Blockage Model for Centrifugal Compressor Impellers", ASME Paper 81-GT-11, 1981.
- 2 Kenny, D. P., "A Novel Correlation of Centrifugal Compressor Performance for Off-Design Prediction", AIAA/ASME/ASE 15th Joint Propulsion Conference, Paper 79-1159, June 1979.
- 3 Johnston, J. P., "The Effects of Rotation on Boundary Layers in Turbomachine Rotors", Fluid Mechanics, Acoustics and Design of Turbomachinery, NASA SP-302, PP. 207-250.
- 4 Rothe, P. H. and Johnston, J. P., "The Effects of System Rotation on Separation, Reattachment and Performance in Two-Dimensional Diffusers", Report PD-17, Thermosciences Division, Dept. Mechanical Engineering, Stanford University, May 1975.
- 5 Sovran, G. and Klomp, E. G., "Experimentally Determined Optimum Geometries for Rectilinear Diffusers with Rectangular, Conical or Annular Cross-section", General Motors Corporation, Warren, Mich., Research Publication GMR-511, November 16, 1965. Fluid Mechanics of Internal Flow, G. Sovran, Ed., Elsevier Publishing Co. 1967.
- 6 Reneau, L. R., Johnston, J. P. and Kline, S. J., "Diffuser Design Manual. Part I - Performance and Design of Straight, Two-Dimensional Diffusers", Report PD-8, Thermosciences Division, Dept. Mechanical Engineering, Stanford University, September 1964.
- 7 Pampreen, R. C. and Musgrave, D. S., "A Method of Calculating the Slip Factor of Centrifugal Compressors from Deviation Angle", Journal of Engineering for Power TRANS ASME, Vol. 100, PP. 121-128, January 1978.